3-(4-Aroyl-1-methyl-1*H*-2-pyrrolyl)-*N*-hydroxy-2-propenamides as a New Class of Synthetic Histone Deacetylase Inhibitors. 2. Effect of Pyrrole-C_2 and/or -C_4 Substitutions on Biological Activity†

Antonello Mai,*,§ Silvio Massa,⊥ Ilaria Cerbara,§ Sergio Valente,§ Rino Ragno,# Patrizia Bottoni,|| Roberto Scatena,|| Peter Loidl,‡ and Gerald Brosch*,‡

Dipartimento di Studi Farmaceutici, Università degli Studi di Roma "La Sapienza", P. le A. Moro 5, 00185 Roma, Italy, Dipartimento Farmaco Chimico Tecnologico, Università degli Studi di Siena, via A. Moro, 53100 Siena, Italy, Dipartimento di Studi di Chimica e Tecnologia delle Sostanze Biologicamente Attive, Università degli Studi di Roma "La Sapienza", P. le A. Moro 5, 00185 Roma, Italy, Istituto di Biochimica e Biochimica Clinica, Università Cattolica del Sacro Cuore, L. go F. Vito 1, 00168 Roma, Italy, and Department of Molecular Biology, University of Innsbruck, Peter-Mayr-Strasse 4b, 6020 Innsbruck, Austria

Received August 6, 2003

Previous SAR studies (Part 1: Mai, A.; et al. *J. Med. Chem.* **2003**, *46*, 512−524) performed on some portions (pyrrole-C_4, pyrrole-N_1, and hydroxamate group) of 3-(4-benzoyl-1-methyl-1*H*-pyrrol-2-yl)-*N*-hydroxy-2-propenamide (**1a**) highlighted its 4-phenylacetyl (**1b**) and 4-cynnamoyl (**1c**) analogues as more potent compounds in inhibiting maize HD2 activity in vitro. In the present paper, we investigated the effect on anti-HD2 activity of chemical substitutions performed on the pyrrole-C_2 ethene chains of **1a**−**c**, which were replaced with methylene, ethylene, substituted ethene, and 1,3-butadiene chains (compounds **2**). Biological results clearly indicated the unsubstituted ethene chain as the best structural motif to get the highest HDAC inhibitory activity, the sole exception to this rule being the introduction of the 1,3-butadienyl moiety into the **1a** chemical structure (IC_{50}(**2f**) = 0.77 μM; IC_{50}(**1a**) = 3.8 μM). IC_{50} values of compounds **3**, prepared as **1b** homologues, revealed that between benzene and carbonyl groups at the pyrrole-C_4 position a hydrocarbon spacer length ranging from two to five methylenes is well accepted by the APHA template, being that **3a** (two methylenes) and **3d** (five methylenes) are more potent (2.3- and 1.4-fold, respectively) than **1b**, while the introduction of a higher number of methylene units (see **3e**,**f**) decreased the inhibitory activities of the derivatives. Particularly, **3a** (IC_{50} = 0.043 μM) showed the same potency as SAHA in inhibiting HD2 in vitro, and it was 3000- and 2.6-fold more potent than sodium valproate and HC-toxin and was 4.3- and 6-fold less potent than trapoxin and TSA, respectively. Finally, conformationally constrained forms of **1b**,**c** (compounds **4**), prepared with the aim to obtain some information potentially useful for a future 3D-QSAR study, showed the same (**4a**,**b**) or higher (**4c**,**d**) HD2 inhibiting activities in comparison with those of the reference drugs. Molecular modeling and docking calculations on the designed compounds performed in parallel with the chemistry work fully supported the synthetic effort and gave insights into the binding mode of the more flexible APHA derivatives (i.e., **3a**). Despite the difference of potency between **1b** and **3a** in the enzyme assay, the two APHA derivatives showed similar antiproliferative and cytodifferentiating activities in vivo on Friends MEL cells, being that **3a** is more potent than **1b** in the differentiation assay only at the highest tested dose (48 μM).

Introduction

Reversible histone acetylation occurring at the ϵ-amino group of lysine residues at the N-terminal tails of core histones mediates conformational changes in nucleosomes. Such modifications affect the accessibility of transcription factors to DNA and regulate gene expression.[1−5] Two classes of enzymes are involved in determining the state of acetylation of histones: histone acetyltransferases (HATs), which catalyze the acetylation of histones acting as transcriptional coactivators, and histone deacetylases (HDACs), which are recruited to the promoter regions by transcriptional repressors and corepressors such as Sin3, SMRT, and N-CoR, leading to hypoacetylated histones.[6−10] Aberrant recruitment of HDACs by oncogenic proteins or a perturbation of the balance between HAT and HDAC activities in normal cells is implicated in malignant diseases.[11−15] HDAC inhibitors (Chart 1), such as the natural products trichostatin A (TSA),[16] trapoxin (TPX),[17] and depsipep-

† Part 1: Mai, A.; Massa, S.; Ragno, R.; Cerbara, I.; Jesacher, F.; Loidl, P.; Brosch, G. 3-(4-Aroyl-1-methyl-1*H*-2-pyrrolyl)-*N*-hydroxy-2-alkylamides as a New Class of Synthetic Histone Deacetylase Inhibitors. 1. Design, Synthesis, Biological Evaluation, and Binding Mode Studies Performed through Three Different Docking Procedures. *J. Med. Chem.* **2003**, *46*, 512−524.

* To whom correspondence should be addressed. For A.M.: (phone) +396-4991-3392; (fax) +396491491; (e-mail) antonello.mai@uniroma1.it. For G.B.: (phone) 0512-507-3608; (fax) 0512-507-2866; (e-mail) gerald.brosch@uibk.ac.at.

§ Dipartimento di Studi Farmaceutici, Università degli Studi di Roma "La Sapienza".

⊥ Università degli Studi di Siena.

Dipartimento di Studi di Chimica e Tecnologia delle Sostanze Biologicamente Attive, Università degli Studi di Roma "La Sapienza".

|| Università Cattolica del Sacro Cuore, Roma.

‡ University of Innsbruck.

10.1021/jm030990+ CCC: $27.50
Published on Web 01/21/2004

Chart 1. Structures of Histone Deacetylase Inhibitors

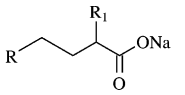

Sodium butyrate (R = R$_1$ = H)
Sodium phenylbutyrate (R = Ph, R$_1$ = H)
Sodium valproate (R = CH$_3$, R$_1$ = *n*-C$_3$H$_7$)

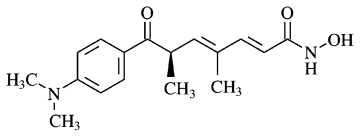

Trichostatin A (TSA)

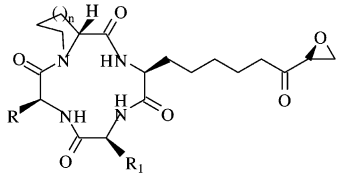

Trapoxin A (TPX) (R = R$_1$ = benzyl, n = 2)
HC-Toxin (R = R$_1$ = methyl, n = 1)

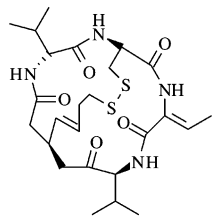

FK-228

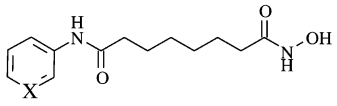

Suberoylanilide hydroxamate (SAHA) (X = CH)
Pyroxamide (X = N)

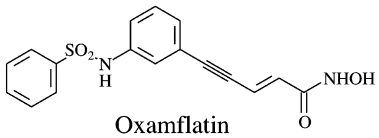

Oxamflatin

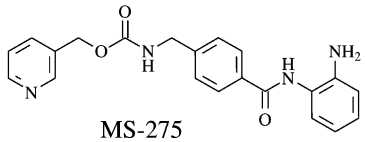

MS-275

tide FK-228,[18] the short-chain fatty acids sodium butyrate,[19] phenylbutyrate,[20] and valproate,[21,22] the hydroxamates suberoylanilide hydroxamic acid (SAHA),[23] pyroxamide, scriptaid,[24] oxamflatin,[25] and cyclic hydroxamic acid containing peptides (CHAPs),[26,27] together with the benzamide MS-275[28,29] are potent inducers of growth arrest, differentiation, or apoptosis in a variety of transformed cells in culture and in animal models.[30−34] Among them, sodium phenylbutyrate (alone or in association with retinoic acid, azacytidine, fluorouracil + indomethacin, or dexamethasone), depsipeptide, SAHA, pyroxamide, and MS-275 are in phase I and/or phase II clinical trials for the treatment of many different cancer diseases.[35] Nevertheless, the clinical benefit of some of them seems to be limited by problems of toxicity (TSA, CHAPs, MS-275), low stability (TSA, trapoxin) and/or solubility (TSA), and low potency and lack of selectivity (butyrates and analogues).[34]

Recently, a new class of synthetic HDAC inhibitors, 3-(4-aroyl-1*H*-pyrrol-2-yl)-*N*-hydroxy-2-propenamides (APHAs), have been described by us.[36−38] The pK_i values of modeled complexes between some aroylpyrrolehydroxyamides previously reported by us as antimicrobial agents[39,40] and archaebacterial HDAC homologues (histone-deacetylase-like protein, HDLP)[41] were predicted in the low (or sub-) micromolar range by an extended VALIDATE 3D QSAR model.[42] Because the inhibiting potencies of other lead HDAC inhibitors were in the submillimolar (sodium valproate),[21,22] micromolar (MS-275),[28,29] or submicromolar (SAHA)[23] range and because of the good agreement between predicted and experimental inhibiting activities of our pyrrole derivatives tested in the enzyme assay against maize histone deacetylase HD2,[43] we chose compound **1a** as the lead

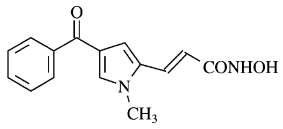

1a

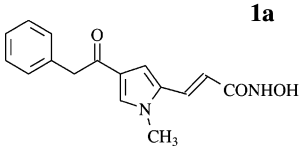

1b

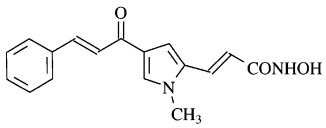

1c

compound of the APHA series. Investigation of the **1a** binding mode into the modeled HDAC1 catalytic core was performed, and its histone hyperacetylation activity on mouse A20 cells was determined.[37] Furthermore, **1a** proved to be effective in growth inhibition (45% and 85% cell growth inhibition at 40 and 80 μM, respectively) and cellular differentiation (18% and 21% of benzidine positive cells at the same concentrations) in murine erythroleukemia (MEL) cells.[37]

Prompted by these findings, we designed chemical modifications on the **1a** structure to determine structure−activity relationships and to improve the HDAC inhibitory effect of APHAs (Figure 1).[38] Replacement of the pyrrole N$_1$-methyl group either with bulkier substituents (isopropyl, phenyl) or with a hydrogen atom led to less potent compounds. Introduction of non-hydroxamate, metal ion complexing moieties at the end of the unsaturated chain linked at the pyrrole-C$_2$ position again furnished weakly potent or totally inac-

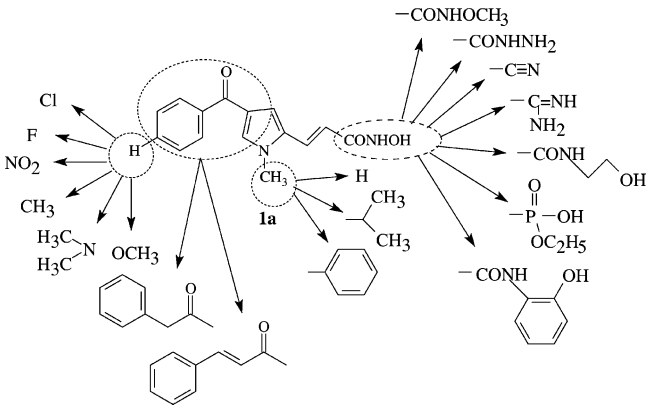

Figure 1. Chemical manipulations[38] performed on lead compound **1a**.

tive derivatives, whereas appropriate C_4-aroyl substitution yielded an increase of inhibitory potency.

Particularly, 3-(1-methyl-4-phenylacetyl-1*H*-pyrrol-2-yl)-*N*-hydroxy-2-propenamide **1b** and 3-[1-methyl-4-(3-phenyl-2-propenoyl)-1*H*-pyrrol-2-yl]-*N*-hydroxy-2-propenamide **1c** were 38- and 3.8-fold more potent than **1a** in the in vitro anti-HD2 assay, respectively.[38]

In the present paper we explore the effect on HDAC inhibiting activity of the replacement of the pyrrole-C_2 ethene moieties of **1a**−**c** with different alkyl/alkenyl chains (compounds **2a**−**s**, Chart 2). Moreover, **1b** homologues with various hydrocarbon linker lengths between the terminal phenyl ring and the carbonyl adjacent to pyrrole ring (compounds **3a**−**f**, Chart 2) have been synthesized and tested as anti-HD2 agents. Finally, conformationally constrained **1b**,**c** analogues (compounds **4a**−**d**, Chart 2) have been synthesized by appropriate C_4-acyl substitutions, with the aim to study the effect of the introduction of conformational restrictions on the APHAs' deacetylase inhibiting activity and to obtain some information potentially useful for a future 3D-QSAR study.

In parallel with the chemistry work, docking studies (Autodock 3.0.5 program)[44,45] on the designed APHA derivatives **2**−**4** into the modeled HDAC1 catalytic binding pocket were performed with the aim of assessing the reliability of the synthetic effort.

Compounds endowed with the best enzyme inhibiting activities have then been evaluated in cell-based assays on antiproliferative and cytodifferentiating effects on Friend MEL cells.

Chemistry

4-Benzoyl-, 4-phenylacetyl-, and 4-cynnammoyl-1-methyl-1*H*-2-pyrrolecarboxaldehydes **5a**−**c**,[38,40] starting materials for the synthesis of title compounds, were treated under Wittig−Horner conditions with the appropriate triethylphosphono esters to give the ethyl 2-substituted 3-pyrrolepropenoates **6d**−**f**,**j**−**o**. Such compounds were converted into the corresponding *N*-hydroxy-2-substituted-3-pyrrolepropenamides **2d**−**f**,**l**−**n**,**q**−**s** by reaction between the 2-substituted 3-pyrrolepropenoic acids **7d**−**f**,**j**−**o**, obtained from **6d**−**f**,**j**−**o** by alkaline hydrolysis, and hydroxylamine via ethoxycarbonyl anhydrides (Scheme 1). *N*-Hydroxy-3-pyrrolepropanamides **2c**,**k** were prepared by catalytic hydrogenation of known 3-(4-benzoyl- and 3-(4-phenylacetyl-1-methyl-1*H*-2-pyrrolyl)-2-propenoic acids[38,40] followed by reaction with hydroxylamine. Base-catalyzed condensation of pyrrolealdehydes **5a**,**b** with malonic acid furnished the pyrroledicarboxylic acids **2g**,**o**, promptly transformed into the corresponding bis-hydroxamides **2h**,**p** (Scheme 1). Friedel−Crafts reaction of methyl 2-pyrroleacetate with benzoyl and phenylacetyl chloride yielded a mixture of isomers, the 2,4-, 2,5-, and 2,3-disubstituted pyrroles (**6a**−**c** and **6g**−**i**) being the reaction products (Scheme 2). Among them, acylpyrroleacetates **6a**,**b**,**g**,**h** were subjected to alkaline hydrolysis and in turn converted into the corresponding hydroxamates **2a**,**b**,**i**,**j** (Scheme 2). Finally the synthesis of compounds **3a**−**f** and **4a**−**d**, which failed using the one-pot Vilsmeier−Haack/Friedel−Crafts method previously reported by us,[36,38−40] was easily accomplished by acylation of ethyl (1-methyl-1*H*-pyrrol-2-yl)propenoate[46] with the appropriate acyl chloride and aluminum trichloride under Friedel−Crafts conditions (Scheme 3). The obtained ethyl 3-(4-acyl-1-methyl-1*H*-pyrrol-2-yl)-2-propenoates **6p**−**y** were then hydrolyzed in alkaline medium and treated with hydroxylamine to afford the desired hydroxamates **3** and **4** (Scheme 3). Chemical and

Chart 2. New Designed APHA Derivatives

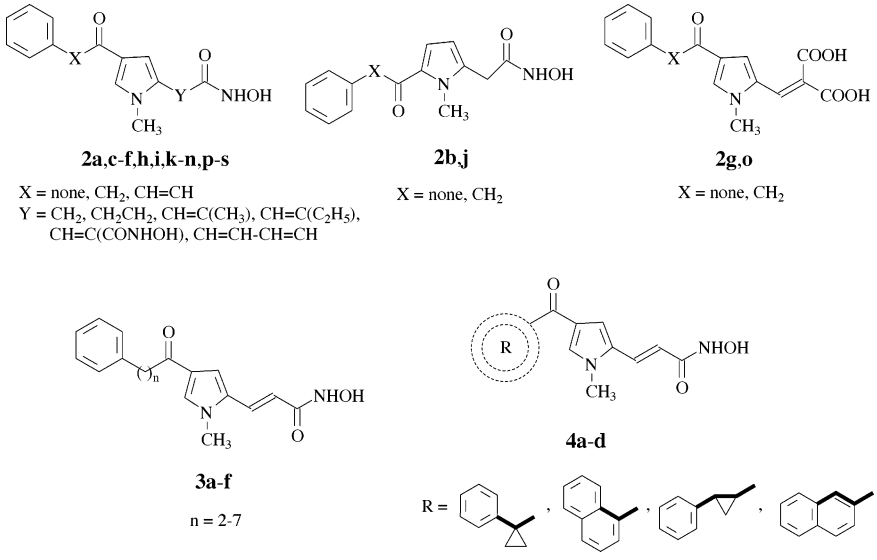

Scheme 1[a]

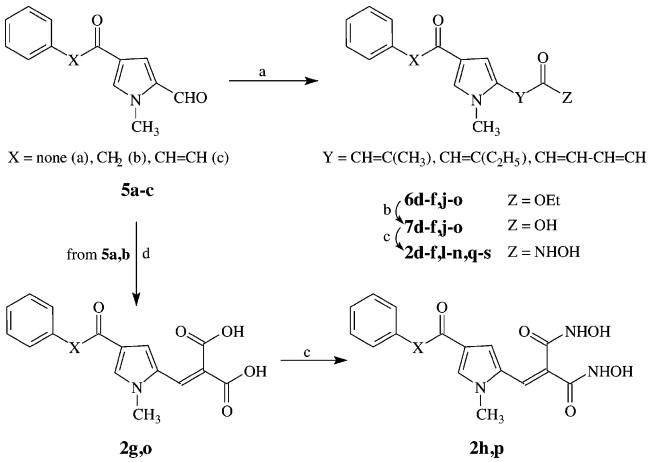

[a] (a) $(C_2H_5O)_2OPCHRCOOC_2H_5$ (R = CH_3, C_2H_5, CH=CH), K_2CO_3, C_2H_5OH, 80 °C; (b) KOH, C_2H_5OH, H_2O, 70 °C; (c) (1) $ClCOOC_2H_5$, $(C_2H_5)_3N$, THF, 0 °C; (2) NH_2OH; (d) malonic acid, aniline, C_2H_5OH, room temp.

Scheme 2[a]

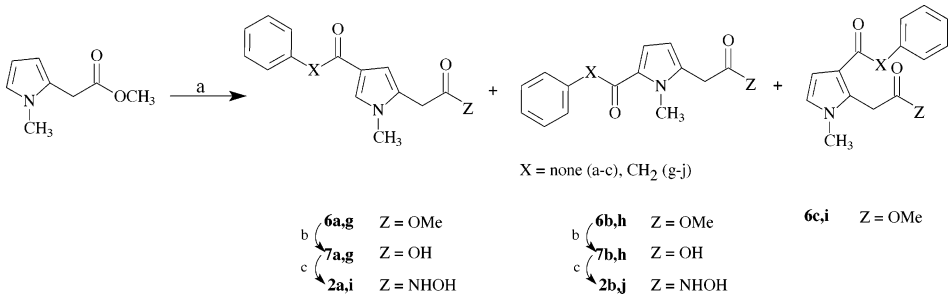

[a] (a) Ph−X−COCl, $AlCl_3$, dichloroethane, room temp; (b) KOH, C_2H_5OH, H_2O, 70 °C; (c) (1) $ClCOOC_2H_5$, $(C_2H_5)_3N$, THF, 0 °C; (2) NH_2OH.

Scheme 3[a]

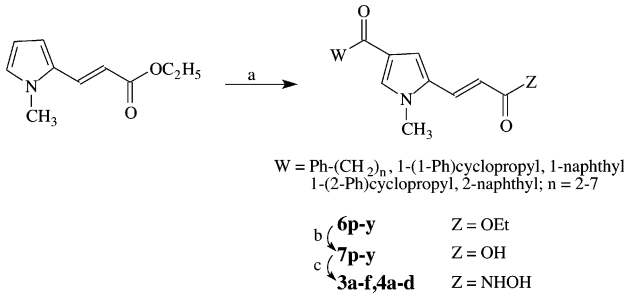

[a] (a) W−COCl (W = Ph−$(CH_2)_n$, 1-(1-Ph)cyclopropyl, 1-naphthyl, 1-(2-Ph)cyclopropyl, 2-naphthyl; n = 2−7), $AlCl_3$, dichloroethane, room temp; (b) KOH, C_2H_5OH, H_2O, 70 °C; (c) (1) $ClCOOC_2H_5$, $(C_2H_5)_3N$, THF, 0 °C; (2) NH_2OH.

physical data of compounds **2**−**4** are listed in Table A (see Supporting Information). Chemical and physical data of intermediate compounds **6** and **7** are listed in Table B (see Supporting Information).

In Vitro Enzyme Inhibition and Structure−Activity Relationships (SARs)

The pyrrole derivatives **2**−**4** were evaluated for their ability to inhibit HDAC activity[47] using maize histone deacetylase HD2 as the enzyme source.[48] Maize HD2[49,51] has an in vitro enzyme activity comparable to those of HDACs from other sources, such as fungi and vertebrates, using our standard HDAC assay.[47,52] Moreover, maize HD2 has been shown to be a good predictive model of mammalian HDACs with various series of HDAC inhibitors.[36−38,53,54]

Two short-chain fatty acids (sodium butyrate and sodium valproate), two hydroxamic acids (TSA and SAHA), and two cyclic tetrapeptides (trapoxin and HC-toxin) were tested together with pyrrole compounds as reference drugs. The results, expressed as the percent of enzyme inhibition at a fixed dose and IC_{50} (50% inhibitory concentration) values, are reported in Table 1. The effects on biological activity of chemical substitutions performed on (i) the ethene chains of **1a**−**c** connecting the aroylpyrrole with the hydroxamate group, (ii) the spacer between benzene and carbonyl groups at the pyrrole-C_4 of **1b**, and (iii) the C_4-aroyl moieties of **1b**,**c** with the production of constrained forms of such compounds are discussed below.

Replacement of 1a−c Ethene Moieties at Pyrrole-C_2 Position with Other (Un)saturated Chains. In the previous paper, 3-(4-benzoyl-1-methyl-1*H*-pyrrol-2-yl)-*N*-hydroxy-2-propenamide **1a**, chosen as the APHA lead compound, was subjected to various chemical manipulations at the pyrrole-C_4 or -N_1 position, as well as to the replacement of hydroxamate moiety with other metal ion complexing groups, with the aim to study the effect of such substitutions on HDAC inhibiting activity.[38] The sole C_4-aroyl substitution of the benzoyl (**1a**) with phenylacetyl (**1b**) or cynnamoyl (**1c**) moieties was successful in improving the anti-HDAC activity, **1b** and **1c** being 38 and 3.8 times more potent than **1a** in the in vitro assay, respectively.[38] In an effort to complete the SAR data on APHA compounds, we replaced the **1a**−**c** ethene chains connecting the pyrrole ring (C_2 position) with the hydroxamate moiety with other

Table 1. HDAC (Maize HD2) Inhibiting Activity of Compounds **2**−**4**[a]

compd	X	*n*	R	Y	% inhibition (at fixed dose (μM))	$IC_{50} \pm SD$ (μM)
2a	none			CH_2	45 (29.8)	34.7 ± 1.0
2b	none				61.3 (29.8)	20.5 ± 0.8
2c	none			CH_2CH_2	45 (33.4)	36.8 ± 1.1
2d	none			$CH{=}C(CH_3)$	83 (27)	2.7 ± 0.08
2e	none			$CH{=}C(C_2H_5)$	37 (25.8)	ND
2f	none			CH=CH−CH=CH	94 (28)	0.77 ± 0.04
2g	none				NI	
2h	none			CH=C(CONHOH)	22.7 (23.3)	66 ± 1.3
2i	CH_2			CH_2	62.8 (28.2)	10.8 ± 0.5
2j	CH_2				64.2 (28.2)	17.1 ± 0.7
2k	CH_2			CH_2CH_2	96 (27)	1.2 ± 0.04
2l	CH_2			$CH{=}C(CH_3)$	95 (26)	1.4 ± 0.03
2m	CH_2			$CH{=}C(C_2H_5)$	NI	
2n	CH_2			CH=CH−CH=CH	89.8 (24.8)	1.48 ± 0.06
2o	CH_2				NI	
2p	CH_2			CH=C(CONHOH)	91 (22.4)	0.2 ± 0.006
2q	CH=CH			$CH{=}C(CH_3)$	96 (25)	1.3 ± 0.05
2r	CH=CH			$CH{=}C(C_2H_5)$	NI	
2s	CH=CH			CH=CH−CH=CH	66 (23.9)	9.9 ± 0.50
3a		2			98 (25.7)	0.043 ± 0.003
3b		3			94 (24.6)	0.13 ± 0.003
3c		4			94 (23.3)	0.11 ± 0.005
3d		5			97.2 (22.6)	0.071 ± 0.003
3e		6			95 (21.7)	0.266 ± 0.013
3f		7			96 (20.8)	0.209 ± 0.008
4a			1-Ph-*c*-Pr		94.2 (21.3)	0.101 ± 0.005
4b			1-naphthyl		93.6 (24)	0.144 ± 0.004
4c			2-Ph-*c*-Pr		97.6 (24.8)	0.31 ± 0.01
4d			2-naphthyl		93.8 (24)	0.115 ± 0.006
1a					86 (33)	3.8 ± 0.15
1b					96 (29)	0.1 ± 0.004
1c					95 (28)	1 ± 0.03
sodium butyrate					35 (5000)	ND
sodium valproate						128 ± 3.8
TSA						0.0072 ± 0.0002
SAHA						0.05 ± 0.0015
trapoxin						0.01 ± 0.0003
HC-toxin						0.11 ± 0.0044

[a] Data points each represent the mean value of at least three separate experiments. NI: no inhibition at starting concentration of 30 μM. ND: not determined.

(un)saturated alkyl chains and we evaluated the effect of such substitutions on enzyme inhibitory activity. *N*-Hydroxypyrroleacetamides **2a**,**b** (**1a** analogues) and **2i**,**j** (**1b** analogues) was from 5 to 170 times less potent than the reference compounds in inhibiting HDAC, and *N*-hydroxypyrrolepropanamides **2c**,**k** showed IC_{50} values 10 times lower than **1a** and **1b**, respectively. The introduction of a methyl substituent at the C_2 position of the **1a**−**c** propenoic chains was well tolerated in the cases of **2d** and **2q** (**1a** and **1c** analogues) [IC_{50}(**2d**) = 2.7 μM; IC_{50}(**2q**) = 1.3 μM; IC_{50}(**1a**) = 3.8 μM; IC_{50}(**1c**) = 1.0 μM], while **2l** (**1b** analogue) was 10 times less active than the unsubstituted counterpart **1b**. Ethyl substitution at the C_2-propenoic chain ruined the anti-HDAC effect of APHA derivatives (see **2e**,**m**,**r**). Replacement of ethene (**1a**−**c**) with 1,3-butadiene (**2f**,**n**,**s**) moieties yielded a significant increase of enzyme inhibiting activity only in the benzoyl series [IC_{50}(**2f**) = 0.77 μM; 5 times more potent than **1a** in in vitro assay], while the phenylacetyl and cynnammoyl derivatives **2n** and **2s** were 10 times less potent than the corresponding references **1b** and **1c**. Pyrrolemethylidenmalonic acids **2g**,**o** failed in inhibiting HDAC activity, while among pyrrole bis-hydroxamates (**2h**,**p**), compound **2p** showed an interesting anti-HDAC activity at submicromolar concentrations, even if lower than that of the monohydroxamate counterpart **1b**.

1b Homologues with Various Hydrocarbon Spacer Lengths. As previously described, the replacement of the C_4 benzoyl moiety of **1a** with a phenylacetyl group led to **1b**, a compound 38-fold more potent than **1a** in HDAC inhibiting activity.[38] On this basis, we explored the effect on biological activity of the insertion of a growing number of methylene units between the terminal phenyl ring and the carbonyl adjacent to the pyrrole ring. Thus, various **1b** homologues (**3a**−**f**) bearing from two to seven methylene units in such positions have been synthesized and tested against HD2. *N*-Hydroxy-3-[1-methyl-4-(3-phenylpropionyl)-1*H*-pyrrol-2-yl]-2-propenamide **3a** was endowed with excellent anti-HDAC activity in the in vitro assay (IC_{50} = 0.043 μM), being 2.3-fold more potent than **1b** and showing the same potency of SAHA in inhibiting the maize HD2 enzyme. In our assay, **3a** was 3000- and 2.6-fold more potent than sodium valproate and HC-toxin and was 4.3- and 6-fold less potent than trapoxin and TSA, respectively. The HD2 inhibitory potency of **1b** homologues with three to five methylene units was well maintained (with **3b**,**c** as active as **1b** and with **3d** 1.4-fold more potent than **1b**), while that shown by six- or seven-methylene-substituted compounds was decreased (see **3e** and **3f**, respectively 2.7- and 2-fold less potent than **1b**).

Conformational Constrained Analogues of 1b,c. Some constrained **1b** analogues (compounds **4a**,**b**) bearing at the pyrrole-C_4 position 1-phenylcyclopropylcarbonyl or 1-naphthoyl moiety as conformationally restricted forms of phenylacetyl, and **1c** analogues (compounds **4c**,**d**) bearing at the pyrrole-C_4 position 2-phenylcyclopropylcarbonyl or 2-naphthoyl moiety as rigid cynnamoyl analogues, have been synthesized and their anti-HDAC activities have been assessed. IC_{50} values showed that enzyme inhibiting activity was well maintained by **4a**,**b**, which showed the same activity as **1b**, and it was improved by **4c** and **4d**, which were 3 and 9 times more potent than **1c** in the in vitro assay.

Molecular Modeling and Docking Studies

Docking studies were performed on all the newly designed APHA derivatives **2**−**4** using our previously reported HDAC1 coordinates modeled from the HDLP structure (PDB entry code 1c3r).[37]

The molecules were drawn by the Macromodel graphical interface Maestro 3.0 using as a template the model of **1a** taken from previous calculations. Initial docking conformations of **2**−**4** were obtained from a simulated annealing run performed in water (GBSA).[55]

From docking studies, three different binding conformations were selected for each docked APHA derivative: (a) the first Autodock scored conformation, herein named "best docked" (BD) conformation; (b) the representative conformation of the most populated cluster, herein named "best cluster" (BC) conformation; (c) the conformation extracted from the lowest energy complex obtained after a single-point minimization of all proposed HDAC1/APHAs complexes by mean of the Macromodel 7.1 program,[56] herein named "best energy" (BE) conformation.

Autodock pK_i values associated with the **2**−**4** selected BE binding conformations are reported in Table 2. The pK_i values obtained by BD and BC conformations are listed in Table C in Supporting Information. For comparison purpose, the same calculations were performed on lead compounds **1a**−**c**.

Data in Table 2 showed a good agreement between predicted pK_i and experimental pIC_{50} values of compounds **2**−**4**, although it is not possible to make a direct correlation between HD2 and HDAC1 inhibitory activities. Nevertheless, considering that the HD2 pIC_{50} value is a close estimation of the HDAC1 pK_i value,[36−38,53,54] the average absolute error of prediction (AAEP) ranged from 0.87 to 1.07, displaying an absolute error of estimation under 1.0 pK_i unit for 54% (BD set), 67% (BC set), and 71% (BE set) of occurrences.

Conformations selected by the BE method are those showing the lowest error of predictions ($AAEP_{BE} = 0.91$). The plot in Figure 2 shows the Autodock pK_i predictions associated with such BE conformations. BD and BC method predictions ($AAEP_{BD} = 1.07$, $AAEP_{BC} = 0.87$) together with mean predictions (AAEP = 0.77) are also reported in Figure A (see Supporting Information).

BE conformations for compounds **1**−**4** in the HDAC1 catalytic pocket are depicted in Figure B (see Supporting Information). Inspection of the APHA's binding mode reveals that the substructure pyrrole-(un)saturated-chain-hydroxamate shows in all molecules almost a unique binding conformation (part A of Figure B), while the pyrrole-C_4 acyl moieties are almost randomly positioned because of the fact that these portions are no longer buried in the enzyme pocket. Interestingly, the orientation of the *N*-methylpyrrole moiety is highly influenced by the chemical nature of the acyl group. Indeed, for APHA derivatives belonging to the aroylpyrrolyl (**1a**, **2a**−**h**), cynnamoylpyrrolyl (**1c**, **2q**−**s**), phen-

Table 2. Experimental Anti-HD2 pIC_{50} and Autodock Predicted (BE Method) Anti-HDAC1 pK_i Values for Compounds **1**−**4**

compd	exptl pIC_{50}[a] (mol/L)	predicted pK_i BE[b] (mol/L)
1a	5.42	6.65
1b	7.00	5.98
1c	6.00	7.08
2a	4.46	5.68
2b	4.69	5.61
2c	4.43	5.55
2d	5.57	5.87
2e	NA[c]	5.15
2f	6.11	3.77
2g	NA[c]	4.79
2h	4.18	3.46
2i	4.97	5.33
2j	4.77	4.79
2k	5.92	6.19
2l	5.85	5.96
2m	NA[c]	6.21
2n	5.83	6.76
2o	NA[c]	5.09
2p	6.70	3.62
2q	5.89	6.64
2r	NA[c]	4.20
2s	5.00	4.32
3a	7.37	6.79
3b	6.89	6.50
3c	6.96	5.39
3d	7.15	6.68
3e	6.58	4.69
3f	6.68	4.27
4a	7.00	6.69
4b	6.84	7.01
4c	6.51	5.95
4d	6.94	6.82
max value	7.37	7.08
min value	4.18	3.46
AAEP		0.91

[a] $pIC_{50} = -\log(IC_{50})$. [b] BE: best energy conformation, the lowest energy from a single-point minimization of the Autodock results (see text). [c] NA: not available.

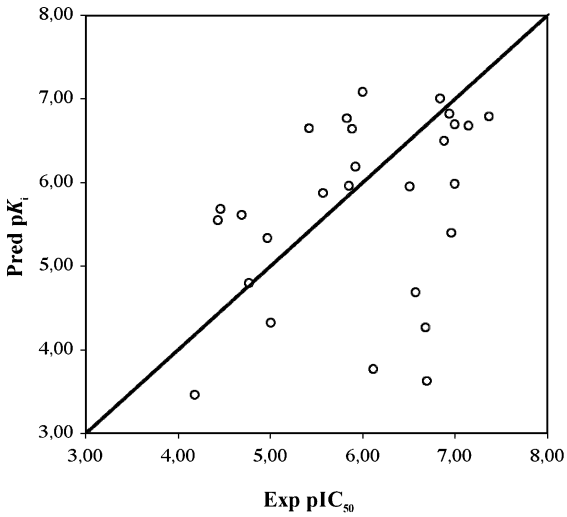

Figure 2. Plot of the Autodock HDAC1 pK_i predictions (BE method) versus the experimental HD2 pIC_{50} values. The black line represents the perfect correlation where $Y = X$.

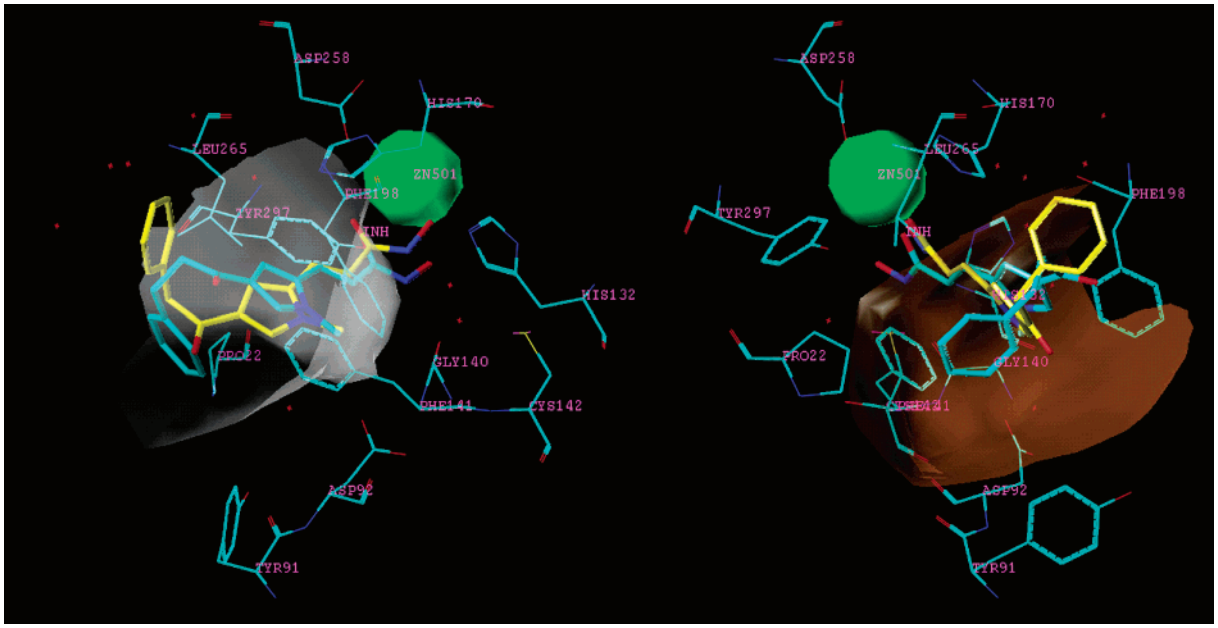

Figure 3. Orthographic view of **1b** (yellow) and **3a** (cyan) binding modes into the HDAC1 catalytic core: (left) shaded in white, the *N*-methylpyrrole binding subpocket; (right) shaded in orange, the pyrrole C4-acyl subsite. The green sphere indicates the Zn ion position in the HDAC1. Hydrogen atoms are not reported for the sake of clarity.

ylpolimethyleneacylpyrrolyl (**3a**−**f**), and conformationally constrained acylpyrrolyl (**4a**−**d**) series (parts B, D, E, and F of Figure B), for 16 molecules out of 23 the *N*-methyl group lies in the same protein cavity, fitting the same area occupied by the C_4-methyl of TSA (not shown). In contrast, with phenylacetylpyrrolyl derivatives **2i**−**p** (part C of Figure B), it is not possible to describe any common binding mode for the *N*-methylpyrrole moiety. In the former group, a further inspection of the seven molecules that do not place the *N*-methyl in the common binding subsite (**2a**,**d**,**g**,**h**,**r**,**s** and **3e**) reveals that for five cases out of seven (**2a**,**g**,**h**,**r**, and **3e**) they correspond to inactive or low-active derivatives. About the remaining two compounds, **2d** (light-green in part B of Figure B) and **2s** (red in part E of Figure B), they showed similar inhibitory activities in comparison with those of the reference compounds **1a** and **1c**. The latter observation agrees with our previous report[38] in which we demonstrated that low-active inhibitors bind in a loose mode, while compounds with higher pIC_{50} display a tighter common binding mode.

An orthogonal view of the **3a** binding mode into the HDAC1 catalytic core is depicted in Figure 3. A comparison between the **3a** binding mode and those described for **1a**[37] and **1b**[38] revealed that the enhancement of inhibitory activity can be mainly attributed to the higher flexibility of the pyrrole-C_4 substituent of **3a**. As previously reported,[38] an increase in flexibility of the chemical structure is unfavorable for binding because of the increase in the entropy. Nevertheless, the introduction of a methylene (**1b**)/ethylene(**3a**) connection between the phenyl and the carbonyl group of the **1a** benzoyl moiety disrupts the extended phenyl−CO−pyrrole π-conjugation. As a consequence of this flexibility, **3a** and to a lesser extent **1b** were found to fit better than **1a** into HDAC1 (**3a**, CO···Zn = 2.87 Å, OH···Zn = 3.01 Å; **1b**, CO···Zn = 3.01 Å, OH···Zn = 3,09 Å; **1a**, CO···Zn = 2.83 Å, OH···Zn = 4.37 Å).

An inspection of **1b** and **3a** binding modes shows that the Gly140 carbonyl group is placed at hydrogen-bond distance from the NH hydroxamate moieties (**1b**, Gly140-CO···$HN_{hydroxamate}$ = 2.65 Å; **3a**, Gly140-CO···$HN_{hydroxamate}$ = 2.77 Å). Positive π-stacking interactions can be observed for both **1b** and **3a** between the pyrrolylethylene chain and the Phe141 and Phe198 residues of the site. Pyrrole N_1-methyl groups of either **1b** or **3a** make favorable interactions with the α-carbon atom of Gly140 and partially with the Phe198 side chain (white area of Figure 3). Finally, the greater difference between **1b** and **3a** is due to the placement of their pyrrole C_4-acyl substituents. The introduction of a further methylene in **3a** enhances the flexibility of this tail, allowing its placement into a hydrophobic cleft made by portions of the side chains of Pro22, Tyr91, Phe141, and Leu265 (orange area of Figure 3), while the carbonyl group points outside the HDAC1 binding pocket, free to make favorable hydrogen bonds with the water environment.

Antiproliferative and Cytodifferentiating Effects of 1b and 3a on Friend MEL Cells. From this study, *N*-hydroxy-3-(1-methyl-4-(3-phenylpropionyl)-1*H*-pyrrol-2-yl)-2-propenamide **3a** emerged as the most potent compound belonging to the APHA series in the in vitro HDAC (HD2) inhibitory assay, with an IC_{50} value of 0.043 μM. This derivative is a homologue (at pyrrole-C_4) of *N*-hydroxy-3-(1-methyl-4-phenylacetyl-1*H*-pyrrol-2-yl)-2-propenamide **1b**, the highly active HDAC inhibitor (IC_{50} = 0.1 μM) chosen as a new lead compound of APHAs.[38] In addition to the in vitro enzyme inhibition assay, the capability of **1b** and **3a** to induce the antiproliferative effect and cell differentiation in Friend MEL cells in vivo has been investigated. Figure 4A shows the effect of the two compounds (**1b**, blue; **3a**, red) on the growth of MEL cells, cultured for 48 h. The compounds showed similar, significant dose-dependent inhibitory effects on the growth rate of the cell line ($p < 0.01$). Interestingly, after 48 h, the inhibitors were not cytotoxic at the tested concentrations (data not shown).

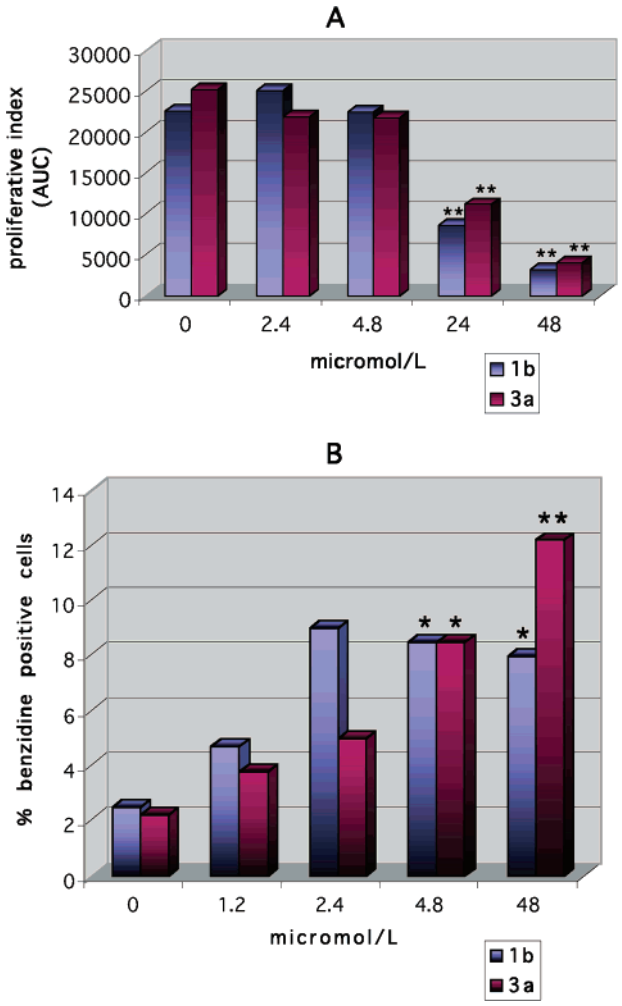

Figure 4. Antiproliferative and cytodifferentiating effects of **1b** and **3a** on MEL cell line. (A) Effects of **1b** (blue) and **3a** (red) on cell growth of MEL cells, cultured for 48 h. Data are expressed as area under the curve (AUC) (mean ± SEM, n = 4): (**) $p < 0.01$. (B) Effects of **1b** (blue) and **3a** (red) on differentiation of MEL cells. The cells were cultured with various concentrations of drugs for 48 h. Each point is the mean ± SEM (n = 4): (*) $p < 0.05$; (**) $p < 0.01$.

In MEL cells, the hemoglobin accumulation, revealed by benzidine staining, is linked to activation of the differentiation process. The results (Figure 4B) clearly indicate a dose-dependent increase of hemoglobin synthesis for both **1b** and **3a** at the tested doses, **3a** being more potent than **1b** as a cytodifferentiating agent at the highest tested concentration (48 μM).

Conclusion

Previous SAR studies performed on some portions (pyrrole-C_4, pyrrole-N_1, and hydroxamate group) of the 3-(4-benzoyl-1-methyl-1*H*-pyrrol-2-yl)-*N*-hydroxy-2-propenamide (**1a**) skeleton highlighted the 4-phenylacetyl (**1b**) and 4-cynnamoyl (**1c**) analogues of **1a** as more potent compounds than **1a** in inhibiting maize HD2 activity in vitro. Docking and binding mode studies performed on **1b** into the modeled HDAC1 catalytic core allow us to explain, in part, the increase of HDAC inhibiting activity from **1a** to **1b**.[38]

In the present paper, we investigated the effect of chemical substitutions performed on the **1a**−**c** pyrrole-C_2 ethene chains, which were replaced with methylene,

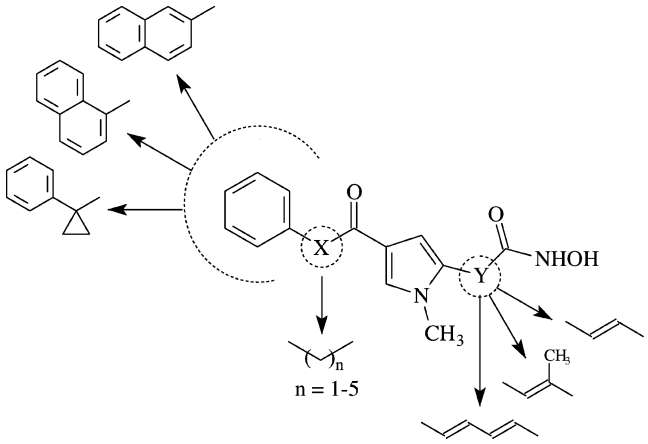

Figure 5. Structural modifications performed on APHA compounds and associated with best HDAC inhibitory activity.

ethylene, substituted ethene, and 1,3-butadiene chains (compounds **2**). Biological results clearly indicated the unsubstituted ethene chain linked at the pyrrole-C_2 position as the best structural motif to get the highest HDAC inhibitory activity, and it was reported with other classes of HDAC inhibitors.[57] The sole exception to this rule is the introduction of the 1,3-butadiene moiety into the **1a** chemical structure, **2f** being 5 times more potent than **1a** in inhibiting HD2 activity. Nevertheless, the same substitution performed on **1b** and **1c** (giving **2n** and **2s**) failed in increasing the anti-HD2 activities of the derivatives, maybe because **2n** and **2s** are too long and too rigid for obtaining suitable accommodation in the enzyme catalytic pocket (Figure 5).

Because the insertion of a methylene between the phenyl and carbonyl groups of **1a** led to **1b**, which is 38-fold more potent, some homologues of **1b** (compounds **3**) bearing a polimethylene spacer at the pyrrole-C_4 acyl portion were synthesized and tested as anti-HDAC agents. IC_{50} values of compounds **3** revealed that a hydrocarbon spacer length ranging from two to five methylene groups is well accepted by the APHA template, being that **3a** (two methylenes) and **3d** (five methylenes) are more potent (2.3- and 1.4-fold, respectively) than **1b**. Introduction of a larger number of methylenes (see **3e** and **3f**, with six and seven methylenes) decreased the inhibitory activities of the derivatives. Finally, conformationally constrained forms of **1b**,**c** (compounds **4**), prepared with the aim to obtain some information potentially useful for a future 3D-QSAR study, showed the same (**4a**,**b**) or higher (**4c**,**d**) HD2 inhibiting activities in comparison with those of the reference drugs **1b**,**c** (Figure 5).

Molecular modeling and docking calculations, performed on the designed APHAs in parallel with the chemical work, fully supported the synthesis and biological evaluation of novel derivatives **2**−**4**. Indeed, more than 75% of these compounds were predicted to have submicromolar activity.

Despite the difference in potency between **1b** (IC_{50} = 0.1 μM) and **3a** (IC_{50} = 0.043 μM) in the enzyme assay, the two APHA derivatives showed similar antiproliferative and cytodifferentiating activities in vivo on Friends MEL cells, **3a** being more potent than **1b** in the differentiation assay only at the highest tested dose (48 μM).

From such findings, a 3D QSAR study on APHA derivatives will be performed to acquire useful data and structural information for structure-based and ligand-based drug design. Moreover, new synthetic efforts will be made to prepare **1b** and **3a** analogues by introducing a variety of substituents at ortho, meta, or para positions of the phenyl ring as well as by replacing the phenyl ring with cycloaliphatic moieties.

Experimental Section

Chemistry. Melting points were determined on a Büchi 530 melting point apparatus and are uncorrected. Infrared (IR) spectra (KBr) were recorded on a Perkin-Elmer Spectrum One instrument. ^{1}H NMR spectra were recorded at 200 MHz on a Bruker AC 200 spectrometer; chemical shifts are reported in δ (ppm) units relative to the internal reference tetramethylsilane (Me_4Si). All compounds were routinely checked by TLC and ^{1}H NMR. TLC was performed on aluminum-backed silica gel plates (Merck DC, Alufolien Kieselgel 60 F_{254}) with spots visualized by UV light. All solvents were reagent grade and, when necessary, were purified and dried by standards methods. Concentration of solutions after reactions and extractions involved the use of a rotary evaporator operating at a reduced pressure of ca. 20 Torr. Organic solutions were dried over anhydrous sodium sulfate. Analytical results are within ±0.40% of the theoretical values. A SAHA sample for biological assays was prepared as previously reported by us.[58] All chemicals were purchased from Aldrich Chimica, Milan (Italy), or from Lancaster Synthesis GmbH, Milan (Italy), and were of the highest purity.

General Procedure for the Synthesis of Methyl Acyl-(1-methyl-1*H*-pyrrol-2-yl)acetates 6a−c,g−i. Example: Methyl (4-Benzoyl-1-methyl-1*H*-pyrrol-2-yl)acetate (2a), Methyl (5-Benzoyl-1-methyl-1*H*-pyrrol-2-yl)acetate (2b), and Methyl (3-Benzoyl-1-methyl-1*H*-pyrrol-2-yl)acetate (2c). Aluminum trichloride (47 mmol, 6.3 g) was slowly added to a cooled (0−5 °C) solution of methyl (1-methyl-1*H*-pyrrol-2-yl)acetate (39.2 mmol, 5.6 mL) and benzoyl chloride (47 mmol, 5.5 mL) in 1,2-dichloroethane (100 mL). After being stirred at room temperature for 30 min, the reaction mixture was poured onto crushed ice (100 g) and the pH of the solution was adjusted to 4 with 37% HCl. The organic layer was separated, and the aqueous one was extracted with chloroform (3 × 50 mL). The combined organic extracts were washed with water (100 mL), dried, and evaporated to dryness. The residual brown oil was purified by column chromatography on silica gel by eluting with a 1:10 mixture of ethyl acetate and chloroform. Three structural isomers have been obtained: the 2,4 isomer (**2a**), which was recrystallized from cyclohexane/benzene; the 2,5 isomer (**2b**), recrystallized from cyclohexane; and the 2,3 isomer (**2c**), recrystallized from cyclohexane/benzene.

2a: ^{1}H NMR ($CDCl_3$) δ 3.65 (s, 3 H, NCH_3), 3.67 (s, 2 H, CH_2 overlapped signal), 3.75 (s, 3 H, OCH_3), 6.62 (m, 1 H, pyrrole β-proton), 7.18 (d, 1 H, pyrrole α-proton), 7.48 (m, 3 H, benzene H-3,4,5), 7.82 (m, 2 H, benzene H-2,6). Anal. ($C_{15}H_{15}NO_3$) C, H, N.

2b: ^{1}H NMR ($CDCl_3$) δ 3.68 (s, 2 H, CH_2), 3.70 (s, 3 H, NCH_3 overlapped signal), 3.92 (s, 3 H, OCH_3), 6.06 (d, 1 H, pyrrole H-3), 6.63 (d, 1 H, pyrrole H-4), 7.42 (m, 3 H, benzene H-3,4,5), 7.76 (m, 2 H, benzene H-2,6). Anal. ($C_{15}H_{15}NO_3$) C, H, N.

2c: ^{1}H NMR ($CDCl_3$) δ 3.65 (s, 3 H, NCH_3), 3.76 (s, 3 H, OCH_3), 4.19 (s, 2 H, CH_2), 6.40 (m, 1 H, pyrrole β-proton), 6.59 (d, 1 H, pyrrole α-proton), 7.48 (m, 3 H, benzene H-3,4,5), 7.82 (m, 2 H, benzene H-2,6). Anal. ($C_{15}H_{15}NO_3$) C, H, N.

General Procedure for the Synthesis of Ethyl (4-Acyl-1-methyl-1*H*-pyrrol-2-yl)alkenoates 6d−f,j−o. Example: Ethyl 3-[4-(3-Phenyl-2-propenoyl)-1-methyl-1*H*-pyrrol-2-yl]-2-ethyl-2-propenoate (6n). A suspension of 4-(3-phenyl-2-propenoyl)-1-methyl-1*H*-pyrrole-2-carboxaldehyde[38] (4.2 mmol, 1.0 g) in absolute ethanol (20 mL) was added in one portion to a mixture of triethyl 2-phosphonobutyrate (5.0 mmol, 1.2 mL) and anhydrous potassium carbonate (12.5 mmol, 1.7 g). After being stirred at 70 °C for 2 h, the reaction mixture was cooled to room temperature and diluted with water (50 mL). The obtained precipitate was filtered and recrystallized from benzene to give pure **6n**. ^{1}H NMR ($CDCl_3$) δ 1.13 (t, 3 H, CH═C−CH_2CH_3), 1.27 (t, 3 H, OCH_2CH_3), 2.58 (q, 2 H, CH═C−CH_2CH_3), 3.67 (s, 3 H, NCH_3), 4.22 (q, 2 H, OCH_2CH_3), 6.98 (d, 1 H, pyrrole β-proton), 7.20 (d, 1 H, pyrrole α-proton), 7.33 (m, 5 H, Ph−CH═CH−CO and benzene H-3,4,5), 7.43 (m, 2 H, benzene H-2,6), 7.75 (d, 1 H, pyrrole−CH═CHCO). Anal. ($C_{21}H_{23}NO_3$) C, H, N.

General Procedure for the Synthesis of Ethyl 3-(4-Acyl-1-methyl-1*H*-pyrrol-2-yl)-2-propenoates 6p−y. Example: Ethyl 3-[1-Methyl-4-(4-phenylbutyryl)-1*H*-pyrrol-2-yl]-2-propenoate (6r). Aluminum trichloride (22.3 mmol, 3.00 g) was slowly added to a cooled (0−5 °C) solution of ethyl 3-(1-methyl-1*H*-pyrrol-2-yl)-2-propenoate[46] (11.2 mmol, 2.0 g) and 4-phenylbutyryl chloride (previously prepared by heating the corresponding acid (22.3 mmol, 3.7 g) with $SOCl_2$ for 1 h at 50 °C) in 1,2-dichloroethane (100 mL). After being stirred at room temperature for 30 min, the reaction mixture was poured onto crushed ice (100 g) and the pH of the solution was adjusted to 4 with 37% HCl. The organic layer was separated, and the aqueous one was extracted with chloroform (3 × 50 mL). The combined organic solution was washed with water (100 mL), dried, and evaporated to dryness. The residual oil was purified by column chromatography on silica gel by eluting with a 1:20 mixture of ethyl acetate and chloroform. Compound **6r** was obtained as a pure oil. ^{1}H NMR ($CDCl_3$) δ 1.37 (t, 3 H, OCH_2CH_3), 2.07 (m, 2 H, $COCH_2CH_2CH_2Ph$), 2.71 (m, 4 H, $COCH_2CH_2CH_2Ph$), 3.76 (s, 3 H, NCH_3), 4.38 (q, 2 H, OCH_2CH_3), 6.27 (d, 1H, CH═CHCO), 7.01 (m, 1 H, pyrrole β-proton), 7.28 (m, 6 H, pyrrole α-proton and benzene H), 7.55 (d, 1 H, CH═CHCO). Anal. ($C_{20}H_{25}NO_3$) C, H, N.

General Procedure for the Synthesis of (4-Acyl-1-methyl-1*H*-pyrrol-2-yl)alkanoic and -alkenoic Acids 7a−y. Example: 5-(1-Methyl-4-phenylacetyl-1*H*-pyrrol-2-yl)-2,4-pentadienoic Acid (7l). A mixture of ethyl 5-(1-methyl-4-phenylacetyl-1*H*-pyrrol-2-yl)-2,4-pentadienoate (**6l**) (4.3 mmol, 1.3 g), 2 N KOH (17.0 mmol, 8.3 mL), and ethanol (15 mL) was heated at 70 °C for 3 h while being stirred. After cooling, the solution was poured into water (50 mL) and extracted with ethyl acetate (3 × 50 mL). A sample of 2 N HCl was added to the aqueous layer until the pH was 5, and the precipitate was filtered and recrystallized from acetonitrile to yield pure **7l**. ^{1}H NMR (DMSO-d_6) δ 3.67 (s, 3 H, NCH_3), 3.97 (s, 2 H, $PhCH_2$), 6.00 (m, 1 H, CH═CH−CH═CH−CO), 6.70 (d, 1H, CH═CH−CH═CH−CO), 7.00 (m, 1 H, pyrrole β-proton), 7.28 (m, 6 H, pyrrole α-proton and benzene H), 7.85 (m, 2 H, CH═CH-CH═CH−CO), 12.15 (bs, 1 H, OH). Anal. ($C_{18}H_{17}NO_3$) C, H, N.

General Procedure for the Synthesis of 3-(4-Acyl-1-methyl-1*H*-pyrrol-2-yl)propanoic Acids 7c,i. Example: 3-(4-Benzoyl-1-methyl-1*H*-pyrrol-2-yl)propanoic Acid (7c). Palladium on active carbon (10%, 0.2 g) was added to a solution of 3-(4-benzoyl-1-methyl-1*H*-pyrrol-2-yl)-2-propenoic acid[40] (2.2 mmol, 0.6 g) in 20 mL of 95% ethanol. The mixture was stirred under H_2 (45 psi) for 3 h and then was filtered to eliminate the catalyst. After evaporation of the solvent, the residual oil was purified by column chromatography on silica gel by eluting with a 1:9 mixture of methanol and chloroform to obtain 0.5 g of a pure solid that was recrystallized from benzene. ^{1}H NMR ($CDCl_3$) δ 2.75 (m, 2 H, CH_2CH_2CO), 2.87 (m, 2 H, CH_2CH_2-CO), 3.59 (s, 3 H, NCH_3), 6.46 (s, 1 H, pyrrole β-proton), 7.10 (s, 1 H, pyrrole α-proton), 7.44 (m, 3 H, benzene H-3,4,5), 7.77 (m, 2 H, benzene H-2,6), 12.10 (bs, 1 H, OH). Anal. ($C_{15}H_{15}$-NO_3) C, H, N.

General Procedure for the Synthesis of (4-Acyl-1-methyl-1*H*-pyrrol-2-yl)-*N*-hydroxyalkanamides and -alkenamides 2a−f,i−n,q−s, 3a−f, and 4a−d. Example: *N*-Hydroxy-3-[1-methyl-4-(5-phenylpentanoyl)-1*H*-pyrrol-2-yl]propenamide (3d). Ethyl chloroformate (2.9 mmol, 0.3 mL) and triethylamine (3.1 mmol, 0.4 mL) were added to a cooled 0 °C solution of **7s** (2.4 mmol, 0.8 g) in dry THF (10 mL), and the mixture was stirred for 10 min. Afterward,

the solid was filtered off and the filtrate was added to a freshly prepared solution of hydroxylamine in methanol, which was obtained from the filtration of the mixture from the reaction between hydroxylamine hydrochloride (3.6 mmol, 0.3 g) and KOH (3.6 mmol, 0.2 g). The resulting mixture was stirred at room temperature for 15 min, then it was evaporated, and the residue was recrystallized from benzene/acetonitrile to afford pure **3d**. ^{1}H NMR (DMSO-d_6) δ 1.58 (m, 4 H, $CH_2CH_2CH_2$-CH_2CO), 2.55 (m, 2 H, $CH_2CH_2CH_2CH_2CO$), 2.68 (m, 2 H, CH_2-$CH_2CH_2CH_2CO$), 3.72 (s, 3 H, NCH_3), 6.25 (d, 1 H, CH=$CHCO$), 6.85 (m, 1 H, pyrrole β-proton), 7.24 (m, 6 H, pyrrole α-proton and benzene H), 7.70 (m, 1 H, CH=CHCO), 8.95 (s, 1 H, NH), 10.65 (s, 1 H, OH). Anal. ($C_{19}H_{22}N_2O_3$) C, H, N.

General Procedure for the Synthesis of 2-(4-Acyl-1-methyl-1*H*-pyrrol-2-yl)methylidenmalonic Acids 2g,o. Example: 2-(4-Benzoyl-1-methyl-1*H*-pyrrol-2-yl)methylidenmalonic Acid (2g). Malonic acid (16.9 mmol, 1.8 g) and aniline (30.9 mmol, 2.9 mL) were added to a solution of 4-benzoyl-1-methyl-1*H*-pyrrole-2-carboxaldehyde[40] (14.1 mmol, 3.0 g) in 20 mL of ethanol. The reaction mixture was stirred at room temperature for 2 h. Afterward, the solution was poured into water (50 mL) and extracted with ethyl acetate (3 × 50 mL). A sample of 2 N HCl was added to the aqueous layer until the pH was 5, and the precipitate was filtered and recrystallized from acetonitrile/ethanol to give pure **2g**. ^{1}H NMR (DMSO-d_6) δ 3.80 (s, 3 H, NCH_3), 7.10 (s, 1 H, pyrrole β-proton), 7.50 (m, 4 H, pyrrole α-proton and benzene H-3,4,5), 7.75 (m, 3 H, benzene H-2,6 and CH=$C(COOH)_2$), 13.05 (bs, 2 H, OH). Anal. ($C_{16}H_{13}NO_5$) C, H, N.

General Procedure for the Synthesis of 2-(4-Acyl-1-methyl-1*H*-pyrrol-2-yl)methyliden-*N*,*N*′-dihydroxymalonamides 2h,p. Example: 2-(1-Methyl-4-phenylacetyl-1*H*-pyrrol-2-yl)methyliden-*N*,*N*′-dihydroxymalonamide (2p). Ethyl chloroformate (22.2 mmol, 2.2 mL) and triethylamine (24.1 mmol, 3.4 mL) were added to a cooled 0 °C solution of **2o** (6.3 mmol, 2.9 g) in dry THF (10 mL), and the mixture was stirred for 10 min. Afterward, the solid was filtered off and the filtrate was added to a freshly prepared solution of hydroxylamine in methanol (obtained from the reaction between hydroxylamine hydrochloride (27.8 mmol, 1.9 g) and KOH (27.8 mmol, 1.6 g)). The resulting mixture was stirred at room temperature for 15 min and was evaporated, and the residue was recrystallized from benzene to yield pure **2p**. ^{1}H NMR (DMSO-d_6) δ 3.71 (s, 3 H, NCH_3), 3.94 (s, 2 H, Ph-CH_2), 6.95 (d, 1 H, pyrrole β-proton), 7.21 (m, 5 H, benzene H), 7.33 (d, 1 H, pyrrole α-proton), 7.96 (d, 1 H, CH=$C(CONHOH)_2$), 9.00 (bs, 2 H, NH), 11.05 (bs, 2 H, OH). Anal. ($C_{17}H_{15}NO_5$) C, H, N.

In Vitro HD2 Enzyme Inhibition. Radioactively labeled chicken core histones were used as the enzyme substrate according to established procedures.[47] The enzyme liberated tritiated acetic acid from the substrate, which was quantified by scintillation counting. IC_{50} values are results of triple determinations. A 50 μL sample of maize enzyme (at 30 °C) was incubated (30 min) with 10 μL of total [^{3}H]acetate-prelabeled chicken reticulocyte histones (1 mg/mL). Reaction was stopped by addition of 36 μL of 1 M HCl/0.4 M acetate and 800 μL of ethyl acetate. After centrifugation (10000*g*, 5 min), an aliquot of 600 μL of the upper phase was counted for radioactivity in 3 mL of liquid scintillation cocktail. The compounds were tested at a starting concentration of 40 μM, and active substances were diluted further. Sodium butyrate, sodium valproate, TSA, SAHA,[58] trapoxin, and HC-toxin were used as the reference compounds, and blank solvents were used as negative controls.

Molecular Modeling and Docking Studies. All molecular modeling calculations and manipulations were performed using the software packages Macromodel 7.1,[56] MOPAC 2000,[59,60] and Autodock 3.0.5[44,45] running on IBM compatible AMD Athlon 2.4 GHz workstations. For the conformational analysis and for any minimization, the all-atom Amber force field[61,62] was adopted as implemented in the Macromodel package. As previously reported[37] the crystal structure of TSA extracted from the HDLP/TSA complex filed in the Brookhaven Protein Data Bank[63] (entry code 1c3r) was used. The HDAC1 model was constructed from HDLP by mutating all the residues comprising a shell of 12 Å from the cocrystallized TSA. Before any docking studies, the HDAC1 model was minimized in a vacuum in the presence of TSA to relieve any steric contact introduced by the mutated residue's side chains.

The binding modes of APHAs **1**−**4** were analyzed by a docking procedure using the program Autodock. For the docking, a grid spacing of 0.375 Å and 58 × 52 × 48 number of points were used. The grid was centered on the mass center of the experimental bound TSA coordinates. The GA-LS method was adopted using the default settings. Amber united atoms were assigned to the protein using the program ADT (Auto Dock Tools). Autodock generated 100 possible binding conformations grouped in clusters.

The **1**−**4** starting conformations for the docking studies were obtained using a molecular dynamic run with simulated annealing procedure as implemented in Macromodel version 7.1 and conducted as follows. Each molecule was energy-minimized to a low gradient. The nonbonded cutoff distances were set to 20 Å for both van der Waals and electrostatic interactions. An initial random velocity to all atoms corresponding to 300 K was applied. Three subsequent molecular dynamics runs were then performed. The first was carried out for 10 ps with a 1.5 fs time step at a constant temperature of 300 K for equilibration purposes. The next molecular dynamic was carried out for 20 ps, during which the system is coupled to a 150 K thermal bath with a time constant of 5 ps. The time constant represents approximately the half-life for equilibration with the bath. Consequently the second molecular dynamic command caused the molecule to slowly cool to approximately 150 K. The third and last dynamic cooled the molecule to 50 K over 20 ps. A final energy minimization was then carried out for 250 iterations using a conjugate gradient. The minimizations and the molecular dynamics were in all cases performed in aqueous solution.

Because of Autodock is not able to perform any energy minimization of the generated complexes, the selection of the binding conformations was not straightforward by using the first Autodock scored conformation. Three binding conformation for each APHA were selected: (a) the first scored Autodock conformation; (b) the most populated cluster representative structure; (c) the lowest energy APHA/HDAC1 complex upon energy-based rescoring of the Autodock cluster representants. The program Macromodel was used to minimize the corresponding Autodock HDAC1/APHA complexes. The ligand and a 10 Å core of atoms of the pocket were allowed to relax during the minimization. An external fixed shell of 8 Å was also included for the long-range interactions. Because of the presence of a metal Zn ion in the HDAC1 catalytic core and the intrinsic molecular mechanic electrostatic limitation of the AMBER force field, the minimizations were performed by applying AM1 charges calculated with the program MOPAC 2000.

Growth Inhibition and Cell Differentiation Assay. Cell Culture and Reagents. Murine erythroleukemia (MEL) cells were obtained from Interlab Cell Line Collection (CBA) (Genoa, Italy). Cells were maintained at 37 °C under a humidified atmosphere of 5% CO_2 in RPMI 1640 Hepes modified medium supplemented with 10% (v/v) heat inactivated fetal calf serum, 2 mmol/L glutamine, 100 IU/mL penicillin, and 100 μg/mL streptomycin. Unless indicated, all chemicals and reagents (cell culture grade) were obtained from Sigma Chemical Co., Milan, Italy.

Cell Viability and Growth Inhibition Assay. Cell number was determined using a Neubauer hemocytometer, and viability was assessed by their ability to exclude trypan blue. The stock solutions were prepared immediately before use. Compounds **1b** and **3a** were dissolved in DMSO. MEL exponentially growing cells (1×10^5 cells/mL) were set at day 0 in media containing various concentrations of drugs for 48 h. The final concentrations of the drugs were 2.4, 4.8, 24, and 48 μM. The final concentration of DMSO, used as a vehicle, was the same (0.1% v/v) in all samples during the experiments. Data

are graphically reported in Figure 4A as area under the curve (AUC) values.

Cytomorphological Assay for MEL Cell Differentiation. The most widely used method for scoring erythroid differentiation is benzidine staining, which reveals the production of hemoglobin.[64] Benzidine dihydrochloride (2 mg/mL) was prepared in 3% acetic acid. Hydrogen peroxide (1%) was added immediately before use. The MEL cell suspensions were mixed with the benzidine solution in a 1:1 ratio and counted in a hemocytometer after 5 min. Blue cells were considered to be positive for hemoglobin.

Statistical Analysis. All results are expressed as the mean ± SEM. The group mean values were compared by analysis of variance (ANOVA) followed by a multiple comparison of means by the Dunnet test. $p < 0.05$ was considered significant.

Acknowledgment. This work was supported by grants from "Progetto Finalizzato Ministero della Salute 2002" (A.M.), "AIRC Proposal 2003" (A.M.), and the Austrian Science Foundation (Grants P13209 (G.B.) and P13620 (P.L.)).

Supporting Information Available: Chemical and physical data for compounds **2**−**4**, **6**, and **7** (Tables A and B) and additional molecular modeling data (Table C, Figures A and B). This material is available free of charge via the Internet at http://pubs.acs.org.

References

(1) Davie, J. R. Covalent modifications of histones: expression from chromatin templates. *Curr. Opin. Genet. Dev*. **1998**, *8*, 173−178.
(2) Kouzarides, T. Histone acetylases and deacetylases in cell proliferation. *Curr. Opin. Genet. Dev*. **1999**, *9*, 40−48.
(3) Strahl, B. D.; Allis, C. D. The language of covalent histone modifications. *Nature* **2000**, *403*, 41−45.
(4) Pazin, M. J.; Kadonaga, J. T. What's up and down with histone deacetylation and transcription? *Cell* **1997**, *89*, 325−328.
(5) Glass, C. K.; Rosenfeld, M. G. The coregulator exchange in transcriptional functions of nuclear receptors. *Genes Dev*. **2000**, *14*, 121−141.
(6) Wu, J.; Grunstein, M. 25 Years after the nucleosome model: chromatin modifications. *Trends Biochem. Sci.* **2000**, *25*, 619−623.
(7) Urnov, F. D.; Wolffe, A. Chromatin organization and human disease. *Emerging Ther. Targets* **2000**, *4*, 665−685.
(8) Luger, K.; Mader, A. W.; Richmond, R. K.; Sargent, D. F.; Richmond, T. J. Crystal structure of the nucleosome core particle at 2.8 Å resolution. *Nature* **1998**, *389*, 251−260.
(9) Grunstein, M. Histone acetylation in chromatin structure and transcription. *Nature* **1997**, *389*, 349−352.
(10) Khochbin, S.; Verdel, A.; Lemercier, C.; Seigneurin-Berny, D. Functional significance of histone deacetylase diversity. *Curr. Opin. Genet. Dev*. **2001**, *11*, 162−166.
(11) Lin, R. J.; Sternsdorf, T.; Tini, M.; Evans, R. M. Transcriptional regulation in acute promyelocytic leukemia. *Oncogene* **2001**, *20*, 7204−7215.
(12) Zelent, A.; Guidez, F.; Melnick, A.; Waxman, S.; Licht, J. D. Translocation of the RARα gene in acute promyelocytic leukemia. *Oncogene* **2001**, *20*, 7186−7203.
(13) Pandolfi, P. P. Transcription therapy for cancer. *Oncogene* **2001**, *20*, 3116−3127.
(14) Grignani, F.; De Matteis, S.; Nervi, C.; Tomassoni, L.; Gelmetti, V.; Cioce, M.; Fanelli, M.; Ruthardt, M.; Ferrara, F. F.; Zamir, I.; Seiser, C.; Grignani, F.; Lazar, M. A.; Minucci, S.; Pelicci, P. G. Fusion proteins of the retinoic acid receptor-α recruit histone deacetylase in promyelocytic leukemia. *Nature* **1998**, *391*, 815−818.
(15) Lutterbach, B.; Westendorf, J. J.; Linggi, B.; Patten, A.; Moniwa, M.; Davie, J. R.; Huynh, K: D.; Bardwell, V. J.; Lavinsky, R. M.; Rosenfeld, M. G.; Glass, C.; Seto, E.; Hiebert, S. W. ETO, a target of t(8;21) in acute leukemia, interacts with the N-CoR and mSin3 corepressors. *Mol. Cell. Biol*. **1998**, *18*, 7176−7184.
(16) Yoshida, M.; Kijima, M.; Akita, M.; Beppu, T. Potent and Specific Inhibition of Mammalian Histone Deacetylase Both in Vivo and in Vitro by Trichostatin A. *J. Biol. Chem*. **1990**, *265*, 17174−17179.
(17) Kijima, M.; Yoshida, M.; Suguta, K.; Horinouchi, S.; Beppu, T. Trapoxin, an Antitumor Cyclic Tetrapeptide, Is an Irreversible Inhibitor of Mammalian Histone Deacetylase. *J. Biol. Chem*. **1993**, *268*, 22429−22435.
(18) Ueda, H.; Nakajima, H.; Hori, Y.; Fujita, T.; Nishimura, M.; Goto, T.; Okuhara, M. FR901228, a novel antitumor bicyclic depsipeptide produced by Chromobacterium violaceum No. 968. I. Taxonomy, fermentation, isolation, physico-chemical and biological properties, and antitumor activity. *J. Antibiot*. **1994**, *47*, 301−310.
(19) Kruh, J. Effects of Sodium Butyrate, a New Pharmacological Agent, on Cells in Culture. *Mol. Cell. Biochem*. **1982**, *42*, 65−82.
(20) Gore, S. D.; Carducci, M. A.; Modifying histones to tame cancer: clinical development of sodium phenylbutyrate and other histone deacetylase inhibitors. *Expert Opin. Invest. Drugs* **2000**, *9*, 2923−2934.
(21) Göttlicher, M.; Minucci, S.; Zhu, P.; Kramer, O. H.; Schimpf, A.; Giavara, S.; Sleeman, J. P.; Lo Coco, F.; Nervi, C.; Pelicci, P. G.; Heinzel, T. Valproic acid defines a novel class of HDAC inhibitors inducing differentiation of transformed cells. *EMBO J*. **2001**, *20*, 6969−6978.
(22) Phiel, C. J.; Zhang, F.; Huang, E. Y.; Guenther, M. G.; Lazar, M. A.; Klein, P. S. Histone deacetylase is a direct target of valproic acid, a potent anticonvulsant, mood stabilizer, and teratogen. *J. Biol. Chem*. **2001**, *76*, 36734−36741.
(23) Richon, V. M.; Emiliani, S.; Verdin, E.; Webb, Y.; Breslow, R.; Rifkind, R. A.; Marks, P. A. A class of hybrid polar inducers of transformed cell differentiation inhibits histone deacetylases. *Proc. Natl. Acad. Sci. U.S.A*. **1998**, *95*, 3003−3007.
(24) Su, G. H.; Sohn, T. A.; Ryu, B.; Kern, S. E. A Novel Histone Deacetylase Inhibitor Identified by High-Throughput Transcriptional Screening of a Compound Library. *Cancer Res*. **2000**, *60*, 3137−3142.
(25) Kim, Y. B.; Lee, K. H., Sugita, K.; Yoshida, M.; Horinouchi, S. Oxamflatin is a novel antitumor compound that inhibits mammalian histone deacetylase. *Oncogene* **1999**, *18*, 2461−2470.
(26) Furumai, R.; Komatsu, Y.; Nishino, N.; Khochbin, S.; Yoshida, M.; Horinouchi, S. Potent histone deacetylase inhibitors built from trichostatin A and cyclic tetrapeptide antibiotics including trapoxin. *Proc. Natl. Acad. Sci. U.S.A*. **2001**, *98*, 87−92.
(27) Komatsu, Y.; Tomizaki, K.; Tsukamoto, M.; Kato, T.; Nishino, N.; Sato, S.; Yamori, T.; Tsuruo, T.; Furumai, R.; Yoshida, M.; Horinouchi, S.; Hayashi, H. Cyclic Hydroxamic-Acid-Containing Peptide 31, a Potent Synthetic Histone Deacetylase Inhibitor with Antitumor Activity. *Cancer Res*. **2001**, *61*, 4459−4466.
(28) Suzuki, T.; Ando, T.; Tsuchiya, K.; Fukazawa, N.; Saito, A.; Mariko, Y.; Yamashita, T.; Nakanishi, O. Synthesis and Histone Deacetylase Inhibitory Activity of New Benzamide Derivatives. *J. Med. Chem*. **1999**, *42*, 3001−3003.
(29) Saito, A.; Yamashita, T.; Mariko, Y.; Nosaka, Y.; Tsuchiya, K.; Ando, T.; Suzuki, T.; Tsuruo, T.; Nakanishi, O. A synthetic inhibitor of histone deacetylase, MS-27-275, with marked in vivo antitumor activity against human tumors. *Proc. Natl. Acad. Sci. U.S.A*. **1999**, *96*, 4592−4597.
(30) Weidle, U. H.; Grossmann, A. Inhibition of Histone Deacetylases: A New Strategy To Target Epigenetic Modifications for Anticamcer Treatment. *Anticancer Res*. **2000**, *20*, 1471−1486.
(31) Kramer, O. H.; Göttlicher, M. G.; Heinzel, T. Histone deacetylase as a therapeutic target. *Trends Endocrinol. Metab*. **2001**, *12*, 294−300.
(32) Marks, P. A.; Richon, V. M.; Breslow, R.; Rifkind, R. A. Histone deacetylase inhibitors as new cancer drugs. *Curr. Opin. Oncol*. **2001**, *13*, 477−483.
(33) Jung, M. Inhibitors of Histone Deacetylase as New Anticancer Agents. *Curr. Med. Chem*. **2001**, *8*, 1505−1511.
(34) Vigushin, D. M.; Coombes, R. C. Histone deacetylase inhibitors in cancer treatment. *Anti-Cancer Drugs* **2001**, *13*, 1−13.
(35) Johnstone, R. W. Histone-deacetylase inhibitors: novel drugs for the treatment of cancer. *Nat. Rev. Drug Discovery* **2002**, *1*, 287−299.
(36) Massa, S.; Mai, A.; Sbardella, G.; Esposito, M.; Ragno, R.; Loidl, P.; Brosch, G. 3-(4-Aroyl-1*H*-pyrrol-2-yl)-*N*-hydroxy-2-propenamides, a New Class of Synthetic Histone Deacetylase Inhibitors. *J. Med. Chem*. **2001**, *44*, 2069−2072.
(37) Mai, A.; Massa, S.; Ragno, R.; Esposito, M.; Sbardella, G.; Nocca, G.; Scatena, R.; Jesacher, F.; Loidl, P.; Brosch, G. Binding Mode Analysis of 3-(4-Benzoyl-1-methyl-1*H*-2-pyrrolyl)-*N*-hydroxy-2-propenamide: A New Synthetic Histone Deacetylase Inhibitor Inducing Histone Hyperacetylation, Growth Inhibition, and Terminal Cell Differentiation. *J. Med. Chem*. **2002**, *45*, 1778−1784.
(38) Mai, A.; Massa, S.; Ragno, R.; Cerbara, I.; Jesacher, F.; Loidl, P.; Brosch, G. 3-(4-Aroyl-1-methyl-1*H*-2-pyrrolyl)-N-hydroxy-2-alkylamides as a New Class of Synthetic Histone Deacetylase Inhibitors. 1. Design, Synthesis, Biological Evaluation, and Binding Mode Studies Performed through Three Different Docking Procedures. *J. Med. Chem*. **2003**, *46*, 512−524.
(39) Corelli, F.; Massa, S.; Stefancich, G.; Mai, A.; Artico, M.; Panico, S.; Simonetti, N. Ricerche su composti antibatterici ed antifungini. Nota VIII. Sintesi ed attività antifungina di derivati

pirrolici correlati con la tricostatina A. (Research on antibacterial and antifungal agents. VIII. Synthesis and antifungal activity of trichostatin A-related pyrrole derivatives.) *Farmaco, Ed. Sci.* **1987**, *42*, 893−903.
(40) Massa, S.; Artico, M.; Corelli, F.; Mai, A.; Di Santo, R.; Cortes, S.; Marongiu, M. E.; Pani, A.; La Colla, P. Synthesis and Antimicrobial and Cytotoxic Activities of Pyrrole-Containing Analogues of Trichostatin A. *J. Med. Chem.* **1990**, *33*, 2845−2849.
(41) Finnin, M. S.; Donigian, J. R.; Cohen, A.; Richon, V. M.; Rifkind, R. A.; Marks, P. A.; Breslow, R.; Pavletich, N. P. Structures of a histone deacetylase homologue bound to the TSA and SAHA inhibitors. *Nature* **1999**, *401*, 188−193.
(42) Head, R. D.; Smythe, M. L.; Oprea, T. I.; Waller, C. L.; Green, S. M.; Marshall, G. R. VALIDATE: A New Method for the Receptor-Based Prediction of Binding Affinities of Novel Ligands. *J. Am. Chem. Soc.* **1996**, *118*, 3959−3969.
(43) Lusser, A.; Brosch, G.; Loidl, A.; Haas, H.; Loidl, P. Identification of maize histone deacetylase HD2 as an acidic nucleolar phosphoprotein. *Science* **1997**, *277*, 88−91.
(44) Goodsell, D. S.; Morris, G. M.; Olson, A. J. Automated docking of flexible ligands: applications of AutoDock. *J. Mol Recognit.* **1996**, *9*, 1−5.
(45) Oshiro, C. M.; Kuntz, I. D.; Dixon, J. S. Flexible ligand docking using a genetic algorithm. *J. Comput.-Aided Mol. Des.* **1995**, *9*, 113−130.
(46) Sinisterra, J. V.; Mouloungui, Z.; Delmas, M.; Gaset, A. Barium hydroxide as catalyst in organic reactions. V. Application in the Horner reaction under solid−liquid phase-transfer conditions. *Synthesis* **1985**, 1097−1100.
(47) Lechner, T.; Lusser, A.; Brosch, G.; Eberharter, A.; Goralik-Schramel, M.; Loidl, P. A comparative study of histone deacetylases of plant, fungal and vertebrate cells. *Biochim. Biophys. Acta* **1996**, *1296*, 181−188.
(48) HD2-activity was extensively purified by anion exchange chromatography (Q-Sepharose), affinity chromatography (Heparin-Sepharose, Histone-Agarose), and size exclusion chromatography (Superdex S200) as described elsewhere.[49,50]
(49) Brosch, G.; Lusser, A.; Goralik-Schramel, M.; Loidl, P. Purification and characterization of a high molecular weight histone deacetylase complex (HD2) of maize embryos. *Biochemistry* **1996**, *35*, 15907−15914.
(50) Kölle, D.; Brosch, G.; Lechner, T.; Lusser, A.; Loidl, P. Biochemical methods for analysis of histone deacetylases. *Methods* **1998**, *15*, 323−331.
(51) Kölle, D.; Brosch, G.; Lechner, T.; Pipal, A.; Helliger, W.; Taplick, J.; Loidl, P. Different types of maize histone deacetylases are distinguished by a highly complex substrate and site specificity. *Biochemistry* **1999**, *38*, 6769−6773.
(52) Brosch, G.; Ransom, R.; Lechner, T.; Walton, J.; Loidl, P. Inhibition of maize histone deacetylases by HC toxin, the host-selective toxin of Cochliobolus carbonum. *Plant Cell* **1995**, *33*, 1941−1950.
(53) Jung, M.; Brosch, G.; Kölle, D.; Scherf, H.; Gerhäuser, C.; Loidl, P. Amide Analogues of Trichostatin A as Inhibitors of Histone Deacetylase and Inducers of Terminal Cell Differentiation. *J. Med. Chem.* **1999**, *42*, 4669−4679.
(54) Wittich, S.; Scherf, H.; Xie, C.; Brosch, G.; Loidl, P.; Gerhäuser, C.; Jumg, M. Structure−Activity Relationships on Phenylalanine-Containing Inhibitors of Histone Deacetylase: In Vitro Enzyme Inhibition, Induction of Differentiation, and Inhibition of Proliferation in Friend Leukemic Cells. *J. Med. Chem.* **2002**, *45*, 3296−3309.
(55) Still, W. C.; Tempczyk, A.; Hawley, R. C.; Hendrickson, T. Semianalytical Treatment of Solvation for Molecular Mechanics and Dynamics. *J. Am. Chem. Soc.* **1990**, *112*, 6127−6129.
(56) Mohamadi, F.; Richards, N. G. J.; Guida, W. C.; Liskamp, R.; Lipton, M.; Caufield, C.; Chang, G.; Hendrickson, T.; Still, W. C. MACROMODEL−an integrated software system for modeling organic and bioorganic molecules using molecular mechanics. *J. Comput. Chem.* **1990**, *11*, 440−467.
(57) Lavoie, R.; Bouchain, G.; Frechette, S.; Woo, S. H.; Khalil, E. A.; Leit, S.; Fournel, M.; Yan, P. T.; Trachy-Bourget, M.-C.; Beaulieu, C.; Li, Z.; Besterman, J. M.; Delorme, D. Design and Synthesis of a Novel Class of Histone Deacetylase Inhibitors. *Bioorg. Med. Chem. Lett.* **2001**, *11*, 2847−2850.
(58) Mai, A.; Esposito, M.; Sbardella, G.; Massa, S. A new facile and expeditious synthesis of *N*-hydroxy-*N*′-phenyloctanediamide, a potent inducer of terminal cytodifferentiation. *Org. Prep. Proced. Int.* **2001**, *33*, 391−394.
(59) Stewart, J. J. MOPAC: a semiempirical molecular orbital program. *J. Comput.-Aided Mol. Des.* **1990**, *4*, 1−105.
(60) *MOPAC 2000.00 Manual*; Stewart, J. J. P., Ed; Fujitsu Limited: Tokyo, Japan 1999.
(61) Pearlman, D. A.; Case, D. A.; Caldwell, J. W.; Ross, W. S.; Cheatham, T. E., III; Debolt, S.; Ferguson, D. M.; Seibel, G. L.; Kollman, P. A. AMBER, a Package of Computer Programs for Applying Molecular Mechanics, Normal-Mode Analysis, Molecular Dynamics and Free Energy Calculations To Simulate the Structural and Energetic Properties of Molecules. *Comput. Phys. Commun.* **1995**, *91*, 1−41.
(62) Pearlman, D. A.; Case, D. A.; Caldwell, J. W.; Ross, W. S.; Cheatham, T. E., III; Ferguson, D. M.; Seibel, G. L.; Singh, U. C.; Weiner, P. K.; Kollman, P. A. *AMBER 4.1*; Department of Pharmaceutical Chemistry, University of California: San Francisco, CA, 1995.
(63) Berman, H. M.; Westbrook, J.; Feng, Z.; Gilliland, G.; Bhat, G. N.; Weissig, H.; Shindyalov, I. N.; Bourne, P. E. The Protein Data Bank. *Nucleic Acids Res.* **2000**, *28*, 235−242.
(64) Rowley, P. T.; Ohlsson-Wilhelm, B. M.; Farley, B. A.; La Bella, S. Inducers of erythroid differentiation in K562 human leukemia cells. *Exp. Hematol.* **1981**, *9*, 32−37.

JM030990+